

Investigating Neutron Polarizabilities through Compton Scattering on  $^3\text{He}$ Deepshikha Choudhury<sup>1</sup>, Andreas Nogga<sup>2</sup> and Daniel R. Phillips<sup>1</sup><sup>1</sup> Department of Physics and Astronomy, Ohio University, Athens, OH 45701,<sup>2</sup> Institut für Kernphysik, Forschungszentrum Jülich, Jülich, Germany

(Dated: May 26, 2019)

We examine manifestations of neutron electromagnetic polarizabilities in coherent Compton scattering from the Helium-3 nucleus. We calculate  $^3\text{He}$  elastic scattering observables using chiral perturbation theory to next-to-leading order ( $\mathcal{O}(e^2 Q)$ ). We find that the unpolarized differential cross section can be used to measure neutron electric and magnetic polarizabilities, while two double-polarization observables are sensitive to different linear combinations of the four neutron spin polarizabilities.

PACS numbers: 13.60.Fz, 25.20.-x, 21.45.+v

The theory that describes the internal dynamics of the neutron is quantum chromodynamics (QCD). The neutron has zero charge, but higher electromagnetic moments encode the strong-interaction dynamics which governs its structure. These quantities therefore provide tests of our understanding of QCD. For example, an early success of the SU(3) quark picture was its prediction of magnetic moments,  $\sim$ , for the neutron and other strongly-interacting particles (hadrons). Magnetic moments are a first-order response to an applied magnetic field. In this paper we will be concerned with electromagnetic polarizabilities, which quantify the second-order response of a particle to electromagnetic fields. The two most basic polarizabilities are the electric and magnetic ones, and  $\sim$ , which measure the ability of an applied electric or magnetic field to produce an induced dipole moment. The Hamiltonian for a neutral particle in applied electric and magnetic fields,  $\mathbf{E}$  and  $\mathbf{B}$ , is then:

$$H = \sim \mathbf{B}^2 - \mathbf{E}^2 + \mathbf{B}^2; \quad (1)$$

where we have worked up to second order in  $\mathbf{E}$  and  $\mathbf{B}$ , and have not yet considered terms which involve derivatives of these fields. For a spin-half particle consideration of such terms allows four new structures which are second order in  $\mathbf{E}$  and  $\mathbf{B}$  [1]. They are:

$$2 \left( \begin{array}{c} h \\ 1 \quad 3 \end{array} \right) \sim \mathbf{E} \cdot \mathbf{E} + \left( \begin{array}{c} i \\ 4 \end{array} \right) \sim \mathbf{B} \cdot \mathbf{B} - \left( \begin{array}{c} z \\ 2 \quad 4 \end{array} \right) \left( \begin{array}{c} i \\ r_i E_j + r_j E_i \end{array} \right) B_j + \left( \begin{array}{c} x \\ 3 \quad i \end{array} \right) \left( \begin{array}{c} r_i B_j + r_j B_i \\ E_j \end{array} \right) \quad (2)$$

The coefficients  $\left( \begin{array}{c} h \\ 1 \quad 3 \end{array} \right)$  are the "spin polarizabilities". This paper will argue that for the neutron, the most basic and stable hadron,  $\sim$ , and  $\left( \begin{array}{c} h \\ 1 \quad 3 \end{array} \right)$  can be extracted from Compton scattering on  $^3\text{He}$ .

Polarizabilities such as those in Eqs. (1) and (2) can be accessed in Compton scattering because the Hamiltonian (1) yields an amplitude for Compton scattering from a neutron target of the form:

$$T_n = \sum_{i=1}^X A_i^{(n)} \left( \begin{array}{c} h \\ 1 \quad 3 \end{array} \right) t_i; \quad (3)$$

Here  $t_1 \{ t_6$  are invariants constructed out of the photon momenta and polarization vectors ( $^0$  and  $^{10}$ ), and, in the case of  $t_3 \{ t_6$ , the neutron spin, e.g.  $t_1 = {}^{10} \wedge$  and  $t_3 = {}^{10} \wedge$ . The  $A_i$ 's are Compton structure functions. The  $!^2$  terms of  $A_1$  and  $A_2$  involve  $\sim$  and  $\left( \begin{array}{c} h \\ 1 \quad 3 \end{array} \right)$ , while the  $!^3$  terms of  $A_3 \{ A_6$  depend on  $\left( \begin{array}{c} h \\ 1 \quad 3 \end{array} \right)$  in various combinations.

For the proton, an expression similar to Eq. (3) but supplemented by the Thomson term,  $\frac{e^2}{M} {}^{10} \wedge$ , applies. The larger cross sections that result from the addition of this term lend themselves to low-energy measurements from which  $^{(p)}$  and  $^{(p)}$  can be extracted. A considerable number of p experiments over the past decade had this as their goal [3]. A combined analysis of their low-energy differential cross section (dcs) data yields [4]:

$$\begin{aligned} {}^{(p)} &= (12.1 \quad 1.1 \text{ (stat.)})^{+0.5}_{-0.5} \text{ (th.)} \quad 10^4 \text{ fm}^3; \\ {}^{(p)} &= (3.4 \quad 1.1 \text{ (stat.)})^{+0.1}_{-0.1} \text{ (th.)} \quad 10^4 \text{ fm}^3; \end{aligned} \quad (4)$$

No elastic Compton scattering measurement of the  $^{(p)}$ 's has yet been performed, but they affect double-polarization observables. Of these,  $z$  and  $x$  are defined by taking the beam helicity to be along  $\hat{z}$ ; then  $z$  ( $x$ ) is the difference between the dcs when the target is spin-polarized along  $+\hat{z}$  ( $+\hat{x}$ ) and along  $-\hat{z}$  ( $-\hat{x}$ ). For  $! < m$  the  $^{(p)}$ 's affect  $z$  and  $x$  because of interference between  $A_3^{(p)} \{ A_6^{(p)}$  and  $A_1^{(p)}$  in the expressions for these observables [5]. An experiment which exploits this interference to probe  $\left( \begin{array}{c} h \\ 1 \quad 3 \end{array} \right)$  has been proposed for the High-Intensity Gamma-ray Source (HIGS) at TUNL [6].

However, neither polarized nor unpolarized Compton scattering experiments can be directly performed on the neutron, since it is not a stable target. A variety of techniques have been proposed to extract  $^{(n)}$  and  $^{(n)}$ , including neutron scattering from the Coulomb field of  $^{208}\text{Pb}$  and Compton scattering on deuteron [7] both elastic and quasi-free. The most accurate numbers come from the last technique and yield (in units of  $10^4 \text{ fm}^3$ ) [7]:

$${}^{(n)} \quad {}^{(n)} = (9.8 \quad 3.6 \text{ (stat.)} \quad 2.2 \text{ (mod.)})^{+2.1}_{-1.1} \text{ (sys.)}; \quad (5)$$

These numbers represent a fascinating interplay of

long-distance ( $r \gg 1/f$ ) and short-distance ( $r \ll 1/f$ ) dynamics. The dominant piece of  $\langle n \rangle$  is due to the "cloud" of virtual pions that surrounds the neutron. But there are also significant contributions from short-distance physics, especially in  $\langle n \rangle$ . This interplay can be systematically computed in baryon chiral perturbation theory (PT), a low-energy effective theory that encodes the low-energy symmetries of QCD and the pattern of their breaking (see Ref. [5] for a review). Observables in PT are computed in an expansion in powers of  $Q = \frac{p \cdot \pi}{E}$ , where  $p$  is the excitation energy of the lightest state not explicitly included in the theory. At  $O(e^2 Q)$  there are no contributions to the  $n$  amplitude from a short-distance  $n$  operator. The prediction for the  $n$  amplitude comes from nucleon-pole, pion-pole, and one-pion-loop diagrams, with the latter capturing the dominant piece of the "pion cloud". This  $O(e^2 Q)$  calculation yields the entire dependence of  $A_1^{(n)}$  ( $A_6^{(n)}$ ) on photon energy and scattering angle up to corrections of  $O(-)$ . The  $O(-^2)$  and  $O(-^3)$  non-pole pieces of  $A_1^{(n)}$  ( $A_6^{(n)}$ ) then give [5, 8]:

$$\langle n \rangle = 10 \langle n \rangle = \frac{5e^2 g_A^2}{384 \pi^2 f^2 m} = 12.2 \cdot 10^{-4} \text{ fm}^3; \quad (6)$$

$$A_1^{(n)} = 2 \langle n \rangle = 4 \langle n \rangle = 4 \langle n \rangle = 4.4 \cdot 10^{-4} \text{ fm}^4; \quad (7)$$

(The  $\langle n \rangle$ 's can also be written in terms of  $g_A$ ,  $f$ , and  $m$ .) The contributions of short-distance physics to Eq. (6) are suppressed by one power of  $Q$ , and to Eq. (7) are suppressed by two powers of  $Q$ . In addition, PT predicts that  $\langle p \rangle$ ,  $\langle p \rangle$ , and the  $\langle n \rangle$ 's are the same as the corresponding neutron quantities at this order. These  $O(e^2 Q)$  predictions of PT agree with the numbers in Eqs. (4) and (5) within the experimental error bars.

We now examine how the predictions of Eqs. (6) and (7) can be tested in  $^3\text{He}$  scattering. The amplitude for this process can be written as

$$M = h_f \hat{p}_f j_{fi}; \quad (8)$$

with  $j_{fi}$  and  $j_f$  anti-symmetrized  $^3\text{He}$  wavefunctions, i.e.  $j_{fi} = (1 + P_{31}P_{12} + P_{32}P_{12})j_{i3}$ , where  $P_{ij}$  is a permutation operator and the subscript on  $j_{i3}$  denotes that nucleon "3" is the spectator. The results quoted in this letter have been calculated using a wavefunction obtained from the Idaho- $N^3\text{LO}$  chiral potential [9] together with the NNLO chiral 3N force [10]. For reviews of PT applied to nuclear forces see Ref. [11].

The operator  $\hat{O}$  in Eq. (8) is the irreducible amplitude for elastic scattering of real photons from the NNN system, calculated in PT up to  $O(e^2 Q)$ . This is next-to-leading order (NLO), a lower order than was used to obtain  $j_{fi}$ , and so our calculation is chirally consistent only to NLO. At NLO  $\hat{O}$  consists of a one-body part

$$\hat{O}^{1B} = \hat{O}^{1B}(1) + \hat{O}^{1B}(2) + \hat{O}^{1B}(3); \quad (9)$$

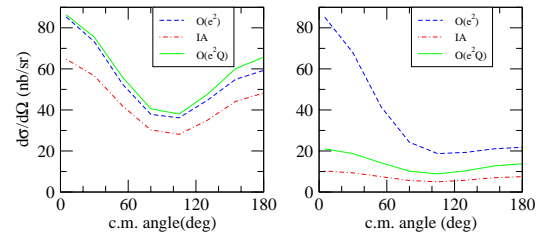


FIG. 1: Comparison of different cm-frame dcs calculations at 60 MeV (left panel) and 120 MeV (right panel).

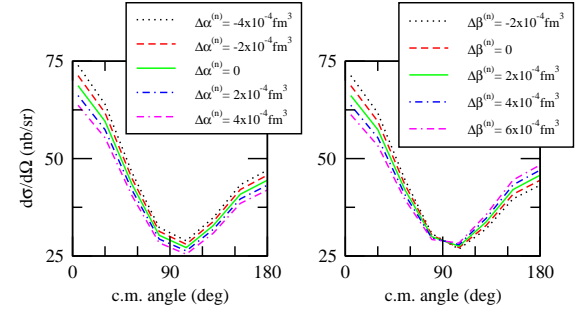


FIG. 2: The cm-frame  $O(e^2 Q)$  dcs at 80 MeV with varying  $\Delta\alpha^{(n)}$  (left panel) and  $\Delta\beta^{(n)}$  (right panel).

with  $\hat{O}^{1B}$  (a) being the  $N$  amplitude where the external photon interacts with nucleon 'a'.  $\hat{O}^{1B}$  (a) (supplemented by what turn out to be very small corrections for the boost from the  $N$  cm. frame to the  $NNN$  cm. frame) follows from Eq. (3) and can be found in Refs. [5, 12]. Meanwhile the two-body part of  $\hat{O}$  is:

$$\hat{O}^{2B} = \hat{O}^{2B}(1;2) + \hat{O}^{2B}(2;3) + \hat{O}^{2B}(3;1); \quad (10)$$

and it represents a sum of two-body mechanisms where the external photons interact with the pair '(a;b)'. At  $O(e^2 Q)$  this operator encodes the physics of two photons coupling to a single pion exchange inside the  $^3\text{He}$  nucleus. (We do not have to include any irreducible three-body Compton mechanisms in our calculation because they appear only at  $O(e^2 Q^3)$ .) We use the expression for  $\hat{O}^{2B}$  given in Ref. [12]. This incorporates the few-nucleon physics that corresponds to the pion-cloud dynamics which yields Eqs. (6) and (7). As such it must be included on an equal footing with the polarizability effects that are our focus. The resulting  $\hat{O}^{2B}$  gives a significant contribution to the total cross section, and is an important piece of the PT calculations that provide a good description of the extant total cross section data [4, 12, 13, 14].

We now simplify Eq. (8) to:

$$M = 3h_f \frac{1}{2} \hat{O}^{1B}(1) + \hat{O}^{1B}(2) + \hat{O}^{2B}(1;2)j_{fi}; \quad (11)$$

using the Faddeev decomposition of  $j_{fi}$ . The structure of the calculation is now similar for the one- and two-body

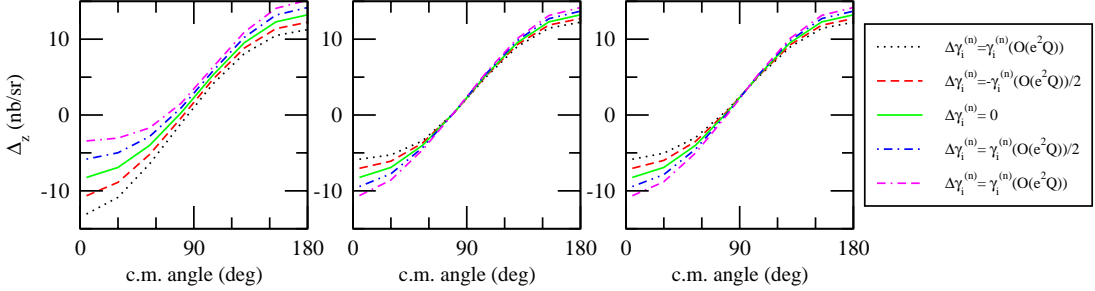


FIG. 3:  $\Delta_z$  at  $\lambda = 120$  MeV with (left-to-right)  $\gamma_1^{(n)}$ ,  $\gamma_2^{(n)}$ , and  $\gamma_4^{(n)}$  varied one at a time. For  $O(e^2 Q)_i^{(n)}$ 's see Eq. (7).

parts. We calculate  $M$  on a partial-wave Jacobi basis. Convergence of the results with respect to the angular momentum expansion was confirmed. For details on the calculational procedure see Ref. [15].

The amplitude (11) is now used to calculate observables. In Fig. 1 we plot our  $O(e^2 Q)$  PT dcs predictions for coherent  $^3\text{He}$  scattering. The two panels are for  $\lambda = 60$  and 120 MeV. Both show three different dcs calculations:  $O(e^2)$ , IA (Impulse Approximation) and  $O(e^2 Q)$ . The  $O(e^2)$  calculation includes only the proton Thomson term, since that is the N amplitude in PT at that order. The IA calculation is done up to  $O(e^2 Q)$  but does not have any two-body contribution. As expected, we see that there is a sizeable difference between the IA and the  $O(e^2 Q)$  dcs: the two-body currents are important and cannot be neglected. Also, we see that the difference between  $O(e^2)$  and  $O(e^2 Q)$  is very small at 60 MeV | PT converges well there| and gradually increases with energy. This is partly because the fractional effect of  $\gamma_1^{(n)}$  and  $\gamma_2^{(n)}$  increases with  $\lambda$ .

To quantify this, in Fig. 2 we plot the  $O(e^2 Q)$  dcs at 80 MeV obtained when we add shifts,  $\gamma_1^{(n)}$  and  $\gamma_2^{(n)}$ , to the  $O(e^2 Q)$  values of the neutron electric and magnetic polarizabilities (6). We take  $\gamma_i^{(n)}$  in the range (4:::4)  $10^{-4}$  fm<sup>3</sup> and  $\gamma_i^{(n)}$  between (2:::6)  $10^{-4}$  fm<sup>3</sup>. This allows us to assess the impact that one set of higher-order mechanisms has on our  $O(e^2 Q)$  predictions. Two features of Fig. 2 are particularly notable. First, sensitivity to  $\gamma_1^{(n)}$  vanishes at  $\theta = 90^\circ$ , so, in principle,  $\gamma_1^{(n)}$  and  $\gamma_2^{(n)}$  can be extracted independently from the same experiment. Second, the absolute size of the shift in the dcs due to  $\gamma_1^{(n)}$  and  $\gamma_2^{(n)}$  is roughly the same for all energies. This suggests that measurements could be done at  $\lambda = 80$  MeV, where the count rate is higher, and the contribution of higher-order terms in the chiral expansion should be smaller.

We have estimated the uncertainty due to short-distance physics in the three-nucleon system by using a variety of  $^3\text{He}$  wave functions generated using various NN interactions with and without a corresponding 3N force. This produced changes of . 15% in the dcs at 120 MeV.

Before examining double-polarization observables in  $^3\text{He}$  scattering we try to develop some intuition for the

$^3\text{He}$  amplitude. Since  $^3\text{He}$  is a spin- $\frac{1}{2}$  target the matrix element (11) can be decomposed in the same fashion as was the neutron's Compton matrix element in Eq. (3).

$$T_{^3\text{He}} = \sum_{i=1}^3 A_i^{^3\text{He}}(\lambda; \theta) t_i; \quad A_i^{^3\text{He}} = A_i^{1B} + A_i^{2B}; \quad (12)$$

where  $A_i^{1B}$  ( $A_i^{2B}$ ) comes from considering the matrix element of the one-body (two-body) operators in Eq. (11), and the structures  $t_3$  ( $t_6$ ) now involve the nuclear| not the neutron| spin. However, in  $^3\text{He}$  the two proton spins are| to a good approximation| anti-aligned, so the nuclear spin is largely carried by the unpaired neutron [16]. We find that the  $O(e^2 Q)$  two-body currents  $A_1^{2B}$  and  $A_2^{2B}$  are numerically sizeable, but  $A_3^{2B}$  ( $A_6^{2B}$ ) are negligible. Hence, to the extent that polarized  $^3\text{He}$  is an effective neutron, we expect  $A_i^{^3\text{He}} = A_i^{(n)}$  for  $i = 3\{6$ . Using Eq. (12) to translate this into predictions for  $\Delta_z$  and  $\Delta_x$  shows that the effects of  $\gamma_1^{(n)}$  {  $\gamma_4^{(n)}$  } will be enhanced in these observables by interference with  $A_1^{^3\text{He}}$ . But  $A_1^{^3\text{He}}$  is| at least at  $\lambda = 80$  MeV| dominated by the contribution of the two protons, and so we anticipate a more marked signal from the neutron spin polarizabilities than is predicted for the corresponding d observables [17].

We emphasize that these arguments are meant only as a guide to the physics of our exact  $O(e^2 Q)$  calculation. Our  $^3\text{He}$  wave function is obtained by solving the Faddeev equations with NN and 3N potentials derived from

PT. All of the effects due to neutron depolarization and the spin-dependent pieces of  $O^{2B}$  are included in our calculation of the amplitude (8). This yields the results for

$\Delta_z$  and  $\Delta_x$  shown in Figs. 3 and 4. There we have proceeded analogously to our computations of the  $^3\text{He}$  dcs, this time varying the neutron spin polarizabilities and seeing the effect on  $\Delta_z$  and  $\Delta_x$ . Fig. 3 indicates that  $\Delta_z$  is quite sensitive to  $\gamma_1^{(n)}$ ,  $\gamma_2^{(n)}$ , and  $\gamma_4^{(n)}$ . With the expected photon flux at an upgraded HIRS such effects can be measured [18]. If this can be done as a function of  $\theta$  we can extract the combination  $\gamma_1^{(n)} + 2\gamma_4^{(n)} \cos \theta$ . Turning to  $\Delta_x$ , Fig. 4 shows that varying  $\gamma_1^{(n)}$  or  $\gamma_4^{(n)}$  produces appreciable effects in  $\Delta_x$  but in a different combination to the sensitivity in  $\Delta_z$ . Use of different  $^3\text{He}$  wave functions alters these predictions for  $\Delta_x$  and

$z$  by  $\sim 7.5\%$ . For a more detailed discussion see [15]. Thus,  $z$  and  $x$  are sensitive to two different linear combinations of  $^{(n)}_1$ ,  $^{(n)}_2$ , and  $^{(n)}_4$  and their measurement should provide an unambiguous extraction of  $^{(n)}_1$ , as well as constraints on  $^{(n)}_2$  and  $^{(n)}_4$ .

These  $^3\text{He}$  scattering calculations are the first calculations for this reaction in any framework. Thus there is significant scope for improvement. An obvious next step is to compute the NNLO ( $O(\epsilon^2 Q^2)$ ) pieces of the NNN operator  $\hat{O}$ . This would allow a more detailed assessment of the pattern of convergence of the effective theory. When this is done we anticipate three kinematic domains where convergence may be somewhat slow. First, since we use the heavy-baryon formulation of PT, the pion-production threshold is at  $! = m$ , rather than in the correct position for  $^3\text{He}$  scattering which is  $4\text{ MeV}$  lower. An estimate of the impact of this discrepancy on observable suggests a  $\sim 5\%$  difference in the dcs, and  $\sim 3\%$  in  $z$  and  $x$ , at  $100\text{ MeV}$ . Second, the power counting used in these calculations is not valid at energies  $\sim \frac{m^2}{M}$ . For instance, it does not reproduce the correct  $! = 0$  (Thomson) limit for the nuclear target, since the terms in  $\hat{O}$  that restore that limit are higher-order effects when  $! \ll m$ . (A recent computation for  $d$  scattering verifies that those terms are indeed a small effect for  $! = 80\text{ MeV}$  [14].) We therefore expect that assessment of these two classes of corrections, while an important check on our results, will not significantly alter them. We believe that the most important correction to focus on is the inclusion of (1232) degrees of freedom in the effective theory. Calculations of  $d$  scattering which included such effects found a sizeable impact on the dcs at backward angles for  $! = 100\text{ MeV}$  [13].

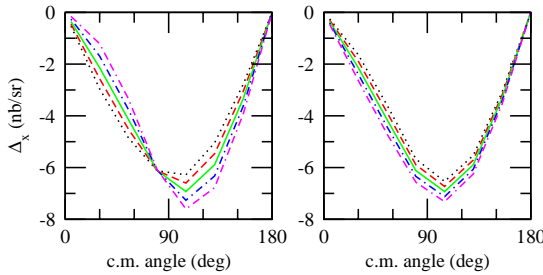


FIG. 4:  $x$  (cm. frame) at  $! = 120\text{ MeV}$  when  $^{(n)}_1$  (left) and  $^{(n)}_4$  (right) are varied one at a time. Legend as in Fig. 3.

Our results for  $^3\text{He}$  scattering are obtained from PT NN & NNN interactions and N & NN operators, and are accurate to NLO in the chiral expansion. These first results on this reaction suggest that  $^{(n)}_1$  and  $^{(n)}_4$  can be extracted from the  $\text{He}^3$  dcs. The resulting  $^{(n)}_1$  and  $^{(n)}_4$  could then be compared to those from  $d$  experiments at MAXLab [19]. Meanwhile, two different linear combinations of  $^{(n)}_1$ ,  $^{(n)}_2$ , and  $^{(n)}_4$  can be constrained by measurements of the double-polarization observables

$z$  and  $x$  at facilities such as HIRIS. Therefore Compton scattering experiments on different targets conducted in concert with further theoretical work should enable accurate extractions of  $^{(n)}_1$  and  $^{(n)}_4$  as well as first experimental results for some neutron spin polarizabilities.

We thank H. Gao, A. Nathan, and L. P. latter for useful conversations. This work was carried out under grant DE-FG 02-93ER 40756 of the U.S. Department of Energy. The numerical calculations for the wavefunctions have been performed at the NIC, Juelich, Germany.

Electronic address: choudhury@phyohiou.edu; Present Address: Department of Physics, George Washington University, Washington, DC 20052.

<sup>y</sup> Electronic address: anogga@fz-juelich.de

<sup>z</sup> Electronic address: philipp@phyohiou.edu

- [1] S. R. Agusa, Phys. Rev. D 47, 3757 (1993); B. R. Holstein, D. D. Recksel, B. Pasquini, M. Vanderhaeghen, Phys. Rev. C 61, 034316 (2000).
- [2] These 'Compton' polarizabilities equal the 'static' ones (Eq. (1)) only in the non-relativistic limit, but the  $\sim 5\%$  difference is understood and calculable.
- [3] For a recent review, see M. Schumacher, Prog. Part. Nucl. Phys. 55, 567 (2005).
- [4] S. R. Beane et al., Phys. Lett. B 567, 200 (2003).
- [5] V. Bernard, N. Kaiser, and Ulf-G. Meißner, Int. J. Mod. Phys. E 4, 193 (1995).
- [6] R. Miskimen, 5th International Workshop on Chiral Dynamics, Theory and Experiment, to appear in the proceedings (World Scientific, Singapore, 2007).
- [7] K. Kossert, et al., Eur. Phys. J., A 16, 259 (2003).
- [8] V. Bernard, N. Kaiser, and Ulf-G. Meißner, Phys. Rev. Lett. 67, 1515 (1991).
- [9] D. R. Entem and R. Machleidt, Phys. Rev. C 68, 041001 (2003).
- [10] U. van Kolck, Phys. Rev., C 49, 2932 (1994); A. Nogga, P. Navratil, B. R. Barrett, and J. P. Vary, Phys. Rev., C 73, 064002 (2006).
- [11] P. F. Bedaque and U. van Kolck, Ann. Rev. Nucl. Part. Sci., 52, 339 (2002); E. Epelbaum, Prog. Part. Nucl. Phys., 57, 654 (2006).
- [12] S. R. Beane, M. M. Alberio, D. R. Phillips, and U. van Kolck, Nucl. Phys. A 656, 367 (1999).
- [13] R. P. Hildebrandt, H. W. Grießhammer, T. R. Hemmert, and D. R. Phillips, Nucl. Phys. A 748, 573 (2005).
- [14] R. P. Hildebrandt, H. W. Grießhammer, and T. R. Hemmert, nucl-th/0512063 (2005).
- [15] D. Choudhury, D. R. Phillips, and A. Nogga, (in preparation); D. Choudhury, Ph.D. Thesis, (2006).
- [16] B. Blankleider and R. M. Woloshyn, Phys. Rev., C 29, 538 (1984); J. L. Friar et al., Phys. Rev., C 42, 2310 (1990).
- [17] D. Choudhury, and D. R. Phillips, Phys. Rev., C 71, 044002 (2005).
- [18] H. Gao, 5th International Workshop on Chiral Dynamics, Theory and Experiment, to appear in the proceedings (World Scientific, Singapore, 2007).
- [19] K. Fissum, ibid.